A Novel Internal Fault Analysis of a Brushless DC Motor Using Winding Function Theory

Hyung-Woo Lee
Dept. of Electrical Engineering
Hanyang University
Seoul, 133-791, Korea

Tae-Hyung Kim
Dept. of Electrical Engineering
Texas A&M University
College Station, TX77843, USA

Changho Choi
R&D center
POSCON Corporation
Seoul, 136-701, Korea

***Abstract*— This paper presents a winding function-based method to analyze the inter-turn fault in stator windings of a Brushless DC (BLDC) motor. It is essential to analyze the behavior of the machine under internal faults and design appropriate protection systems to avoid expensive failures. The winding functions and inductance of stator windings will be explained in detail and the informative simulation results based on the winding function theory will be provided to analyze currents abnormalities and torque pulsation under turn-to-turn short. Analytical consideration of the stator currents and torque waveform of both healthy and faulty machine is also developed. The detailed simulation results of this paper will be the guideline for early detection of internal failures in BLDC motors.**

Keywords - BLDC Motor; Internal fault analysis; Turn-to- turn short; Winding function theory

I. INTRODUCTION

Electric motors play a very important role in the safe and efficient running of industrial plants and processes. The adverse conditions of heat and vibration are naturally exposed and will occasionally lead to the progressive deterioration and eventual breakdown of the winding insulation in a phase of the machine. This internal fault will increase torque ripple that deteriorates machine performance. Understanding and early detection of abnormalities in the motors will help to avoid expensive failures.

Many researches [1]-[5] indicate that the majority of motor stator winding failures result from breakdown of the turn-to-turn insulation. Although there is no experimental data to indicate the time delay between inter-turn and ground wall insulation failure, it is probable that the transition between the two states is not instantaneous. Therefore, early detection of inter-turn shorts especially, turn-to-turn shorts of winding during motor operation would eliminate subsequent damage to adjacent coils and the stator core, reducing repair cost and motor outage time.

In this paper, a winding function-based method for modeling a BLDC motor with turn-to-turn short circuit in the stator winding is developed and this new approach to the internal fault analysis will help to understand the effect of the turn-to-turn short and be the guideline for early detection of internal failures in BLDC motors.

II. CHARACTERISTICS AND OPERATIONAL PRINCIPLE OF THE BLDC MOTOR

The BLDC motor is essentially configured as a permanent magnet rotating machine that has a set of current-carrying conductors. In this respect it is equivalent to an inverted DC commutator motor, in that the magnet rotates while the conductors remain stationary. In both cases, the current in the conductors must reverse polarity when a magnet pole passes by, in order to keep the unidirectional torque. In the DC commutator motor, the commutator and brushes perform the polarity reversal. Since the commutator is fixed to the rotor, the switching instants are automatically synchronized with the alternating of the magnetic field through which the conductors are passing. In the BLDC motor, the polarity reversal is performed by power transistors, which must be switched in synchronism with the rotor position. The process of commutation is similar in the two machines, and the resulting performance equations and speed/torque characteristics are almost identical. Fig. 1 shows the cross sectional view of the three-phase BLDC motor, which has four poles.

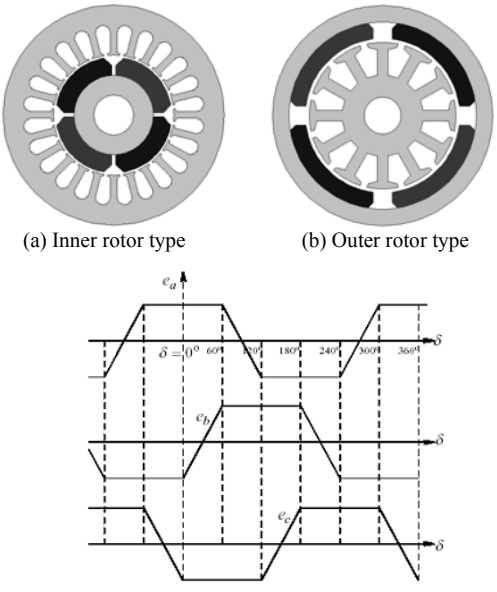

(a) Inner rotor type (b) Outer rotor type

(c) Three-phase induced EMF

Fig. 1. Cross sectional view of the BLDC motor and induced EMF.

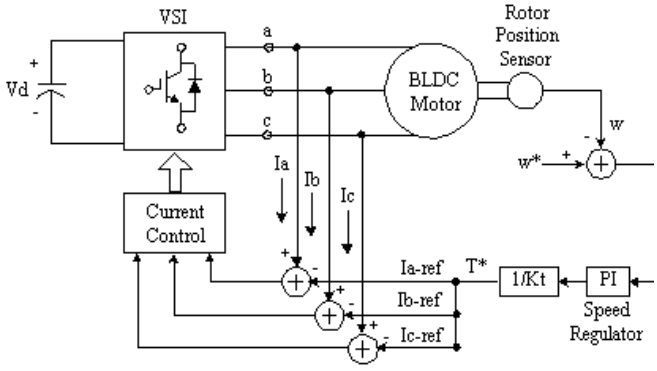

Fig. 2. Block diagram of speed and torque control.

As the rotor rotates, the trapezoidal EMF (Electro-Motive Force) is induced in the stator winding as shown in Fig. 1(c). This non-sinusoidal EMF is due to the concentric winding of the machine and rectangular distribution of the magnetic flux in the airgap [6]. Based on the trapezoidal back EMF waveforms, the inverter should be controlled to generate the 120° conducting current profile, which is synchronized in the flat part of the EMF profile, to generate the constant torque. Using PWM current control scheme, the speed and torque control is possible with a position sensor, such as hall sensor or encoder as shown in Fig. 2.

III. Numerical Expression using Winding Function Theory under Stator Turn-to-turn Fault

A. Winding functions in healthy case

Fig. 3(a) shows the winding placement of phase A in a healthy motor, and other phase B and C will be located in the position 120, 240 electrical degree apart from phase A respectively. Turn functions of each phase are shown in Fig. 3(b). In the healthy condition, winding functions [1] of 4-pole BLDC motors are as (1):

$$N_A = \frac{N}{\pi}[\cos\varphi - \frac{1}{3}\cos 3\varphi + \frac{1}{5}\cos 5\varphi - .....]$$
$$N_B = \frac{N}{\pi}[\cos(\varphi - \frac{2\pi}{3}) - \frac{1}{3}\cos 3(\varphi - \frac{2\pi}{3}) + \frac{1}{5}\cos 5(\varphi - \frac{2\pi}{3}) - .....] \quad (1)$$
$$N_C = \frac{N}{\pi}[\cos(\varphi + \frac{2\pi}{3}) - \frac{1}{3}\cos 3(\varphi + \frac{2\pi}{3}) + \frac{1}{5}\cos 5(\varphi + \frac{2\pi}{3}) - .....]$$

where, N is the number of turns.

B. Winding functions and inductance under internal fault

Winding configuration in case of turn-to-turn fault (1 turn fault) in one phase is shown in Fig. 4(a). In this case, there will be a short circuit following the thick line and the short circuit currents flow in opposite direction. Fig. 4(b) shows the winding placement of phase A and short circuit (A_{sc}) in this case.

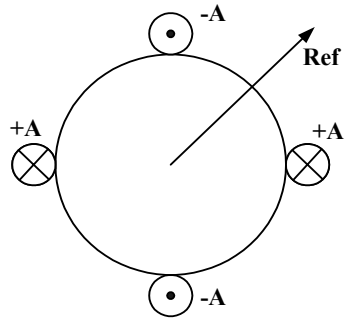

(a) Winding placement of phase A

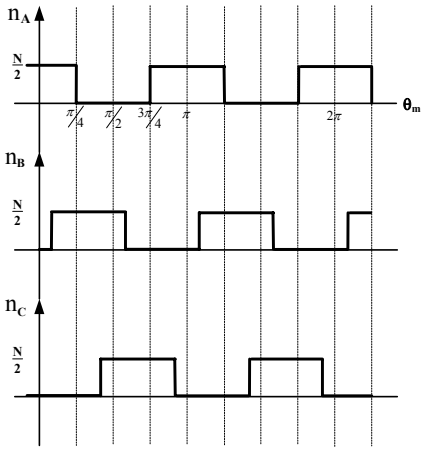

(b) Turn functions of each phase

Fig. 3. Healthy motor case.

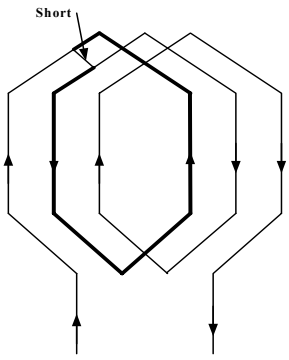

(a) Winding configuration of turn-to-turn short

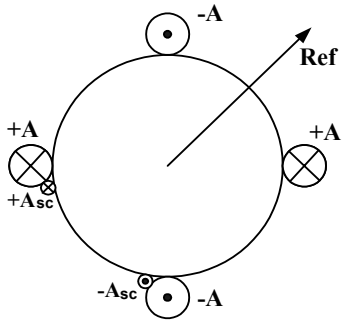

(b) Winding placement of phase A and short circuit

Fig. 4. Internal fault case.

Turn functions and winding functions of each phase and short circuit are shown in Fig. 5 through Fig. 11. Under the 10% turn-to-turn fault (4-pole, 50turns case), self and mutual inductance are calculated based on winding function theory and are utilized for voltage equation. Calculated inductance between each phase and short circuit are also presented in (2) through (8).

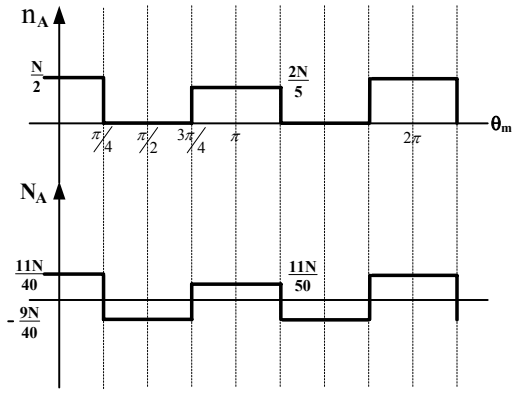

Fig. 5. Turn function and winding function of phase A under the 10% turn-to-turn fault (4-pole, 50turns case).

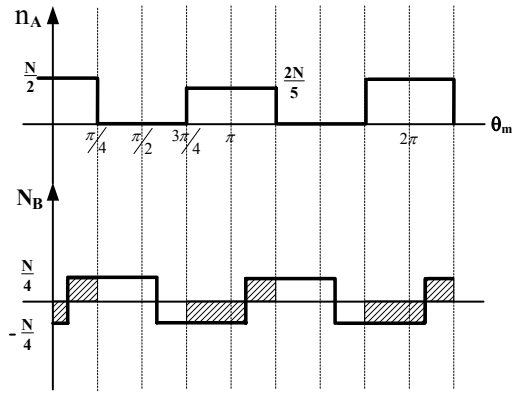

Fig. 6. Turn function and winding function of phase A and B.

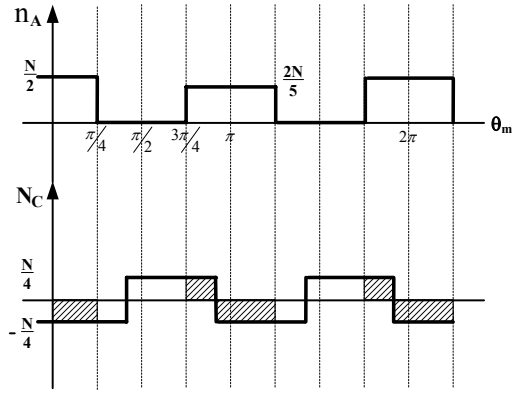

Fig. 7. Turn function and winding function of phase A and C.

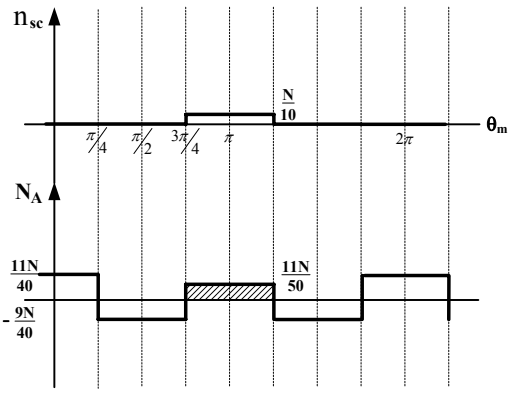

Fig. 8. Turn function of short circuit in phase A and winding function of phase A.

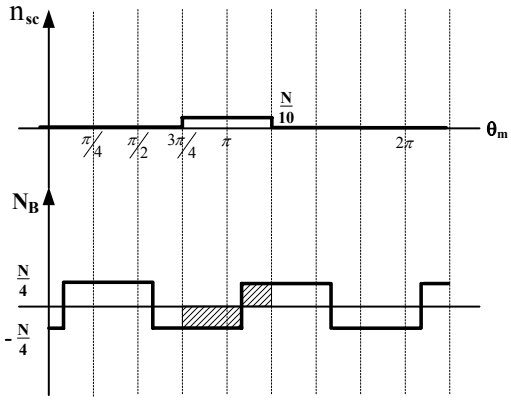

Fig. 9. Turn function of short circuit in phase A and winding function of phase B.

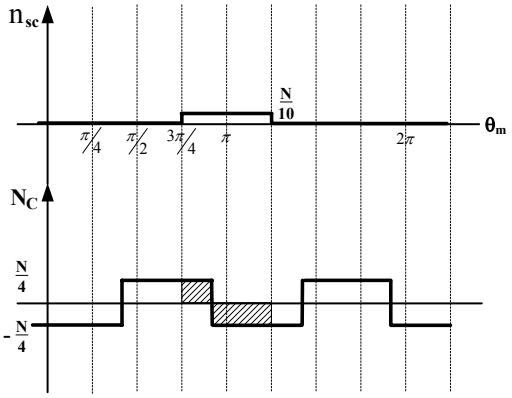

Fig. 10. Turn function of short circuit in phase A and winding function of phase C.

$$L_{AA} = \frac{\mu_o rl}{g}[\int_0^{2\pi} n_A(\theta) N_A(\theta) d\theta] = \frac{\mu_o rl\pi N^2}{80000g}[3x^2 - 200x + 10000] \quad (2)$$

(x : internal fault ratio; x=10 at 10% turn-to-turn fault)

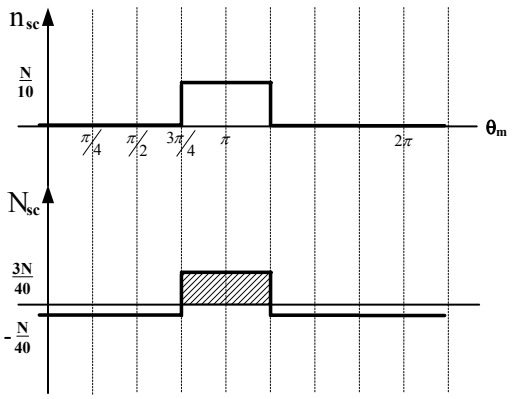

Fig. 11. Turn function and winding function of short circuit in phase A.

$$L_{BB} = \frac{\mu_o rl}{g}[\int_0^{2\pi} n_B(\theta) N_B(\theta) d\theta]$$

$$L_{CC} = \frac{\mu_o rl}{g}[\int_0^{2\pi} n_C(\theta) N_C(\theta) d\theta] = \frac{\mu_o rl\pi N^2}{8g} = L_{BB} \quad (3)$$

$$L_{AB} = \frac{\mu_o rl}{g}[\int_0^{2\pi} n_A(\theta) N_B(\theta) d\theta] = -\frac{\mu_o rl\pi N^2}{2400g}[100 - x] = L_{BA} = L_{AC} = L_{CA} \quad (4)$$

$$L_{BC} = \frac{\mu_o rl}{g}[\int_0^{2\pi} n_B(\theta) N_C(\theta) d\theta] = -\frac{\mu_o rl\pi N^2}{24g} = L_{CB} \quad (5)$$

$$L_{SCA} = \frac{\mu_o rl}{g}[\int_0^{2\pi} n_{SC}(\theta) N_A(\theta) d\theta] = \frac{\mu_o rl\pi N^2}{80000g}[3x^2 - 100x] = L_{ASC} \quad (6)$$

$$L_{SCB} = \frac{\mu_o rl}{g}[\int_0^{2\pi} n_{SC}(\theta) N_B(\theta) d\theta] = \frac{\mu_o rl\pi N^2}{2400g}[x] = L_{BSC} = L_{CSC} = L_{SCC} \quad (7)$$

$$L_{SCSC} = \frac{\mu_o rl}{g}[\int_0^{2\pi} n_{SC}(\theta) N_{SC}(\theta) d\theta] = \frac{\mu_o rl\pi N^2}{80000g}[3x^2] \quad (8)$$

L_{XY} : Mutual inductance between phase X and phase Y
L_{XX} : Self inductance of phase X
- X and Y can be A, B, C and sc (short circuit)
μ_o : permeability of free space
r : radius of the rotor
l : stack length
g : airgap + permanent magnet thickness

C. Voltage equation

From the calculated self and mutual inductances between each phase and short circuit, the corresponding voltage equations of a Brushless DC motor under stator turn-to-turn faults can be expressed as in (9). These voltage equations are used for the internal fault analysis of a BLDC motor.

$$\begin{aligned} V_a &= RI_a + L_{aa}\frac{dI_a}{dt} + L_{ab}\frac{dI_b}{dt} + L_{ac}\frac{dI_c}{dt} + L_{asc}\frac{dI_{sc}}{dt} + E_a \\ V_b &= RI_b + L_{ba}\frac{dI_a}{dt} + L_{bb}\frac{dI_b}{dt} + L_{bc}\frac{dI_c}{dt} + L_{bsc}\frac{dI_{sc}}{dt} + E_b \\ V_c &= RI_c + L_{ca}\frac{dI_a}{dt} + L_{cb}\frac{dI_b}{dt} + L_{cc}\frac{dI_c}{dt} + L_{\mathrm{csc}}\frac{dI_{sc}}{dt} + E_c \\ 0 &= R_{sc}I_{sc} + L_{sca}\frac{dI_a}{dt} + L_{scb}\frac{dI_b}{dt} + L_{scc}\frac{dI_c}{dt} + L_{s\,\mathrm{csc}}\frac{dI_{sc}}{dt} + E_{sc} \end{aligned} \quad (9)$$

where, Back EMF is

$$\begin{aligned} E_a &= \pi^2 (Dl) f \sum_{n=1}^{\infty} N_a B_n \cos[n(wt)] \\ E_b &= \pi^2 (Dl) f \sum_{n=1}^{\infty} N_b B_n \cos[n(wt - \frac{2\pi}{3})] \\ E_c &= \pi^2 (Dl) f \sum_{n=1}^{\infty} N_c B_n \cos[n(wt + \frac{2\pi}{3})] \\ E_{sc} &= \pi^2 (Dl) f \sum_{n=1}^{\infty} N_{sc} B_n \cos[n(wt)] \end{aligned} \quad (10)$$

where, R, f, and B_n are phase resistance, operating frequency, and flux density, respectively.

Based on (9) and (10), dynamic equations for simulation are given as (11):

$$\begin{bmatrix} \frac{dIa}{dt} \\ \frac{dIb}{dt} \\ \frac{dIc}{dt} \\ \frac{dIsc}{dt} \end{bmatrix} = \begin{bmatrix} L_{aa} & L_{ab} & L_{ac} & L_{asc} \\ L_{ba} & L_{bb} & L_{bc} & L_{bsc} \\ L_{ca} & L_{cb} & L_{cc} & L_{\mathrm{csc}} \\ L_{sca} & L_{scb} & L_{scc} & L_{s\,\mathrm{csc}} \end{bmatrix}^{-1} \left(\begin{bmatrix} V_a \\ V_b \\ V_c \\ 0 \end{bmatrix} - \begin{bmatrix} E_a \\ E_b \\ E_c \\ E_{sc} \end{bmatrix} - \begin{bmatrix} RI_a \\ RI_b \\ RI_c \\ R_{sc}I_{sc} \end{bmatrix} \right) \quad (11)$$

IV. Results of the Internal Fault Analysis

Table I shows the specification of the 4-pole BLDC motor used in the analysis. It is assumed that the stator turn-to-turn short is occurred at t = 0.7[sec]. From 0 to 0.7[sec], motor runs under healthy condition with closed-loop PWM speed control (PI control), and from 0.7 to 0.76[sec], motor runs under turn-to-turn short condition. When the internal fault occurs, the short current will flow through the short circuit.

TABLE I
BLDC MOTOR SPECIFICATION

Phase	3	Rated Power	300[*W*]
Rated Current	4[*A*]	Rated Speed	3000[*RPM*]
Resistance	4[Ω]	K_e	0.215[*V/rps*]
Stack length	100[*mm*]	g	2.5[*mm*]
Inertia (*J*)	1.141[gm^2]	# of turn	50

Fig. 12 shows the simulation results when one turn of phase A winding is shorted. Even though just one turn-to-turn short is occurred, around 20[A] maximum short circuit current is flowing in the short circuit at commutation points. This large amount of short circuit current can easily cause break-down of the adjacent winding insulation. Fig. 13 and 14 show the simulation results when the internal turn-to-turn fault ratio increases as 30[%] and 50[%]. In these situations, back-EMF in phase A decreases since the induced voltage is proportional to the number of turns, and phase currents waveforms deform gradually. Consequently, torque ripple become worse. From the simulation results, it is certain that even a single turn-to-turn fault can result in short current that is much larger than rated currents, and the fault is likely to propagate into whole stator winding rapidly if no action is taken.

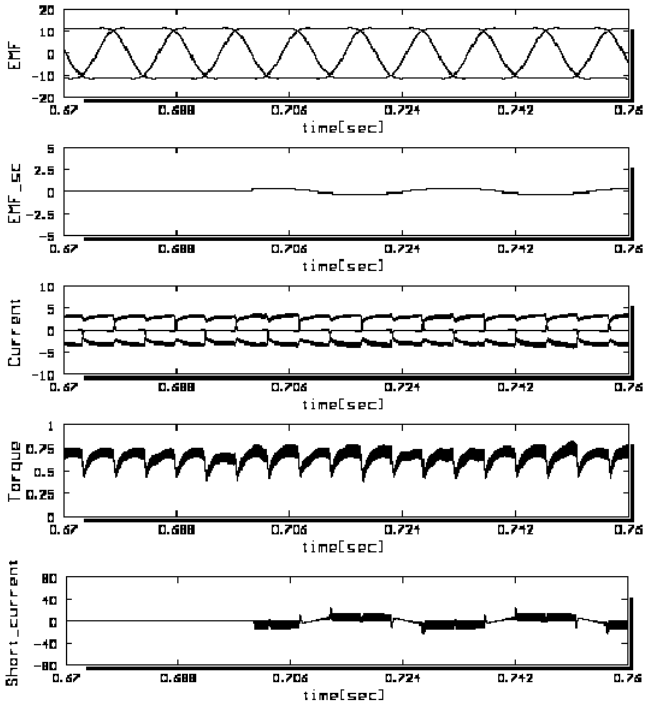

Fig. 12. Waveforms during healthy case (0.67~0.7[sec]) and one turn short circuit case (0.7~0.76[sec]).
(a) Phase EMFs (b) Short circuit EMF (c) Phase currents (d) Torque (e) Short circuit current

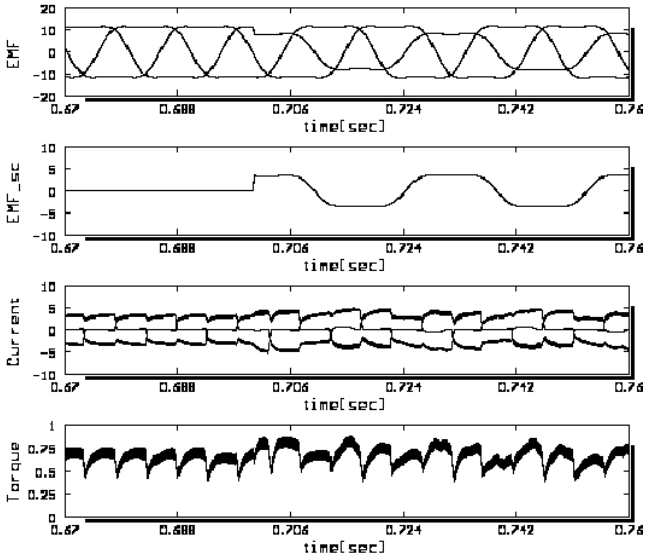

Fig. 13. Waveforms during healthy case (0.67~0.7[sec]) and 30% turn-to-turn fault case (0.7~0.76[sec]).
(a) Phase EMFs (b) Short circuit EMF (c) Phase currents (d) Torque

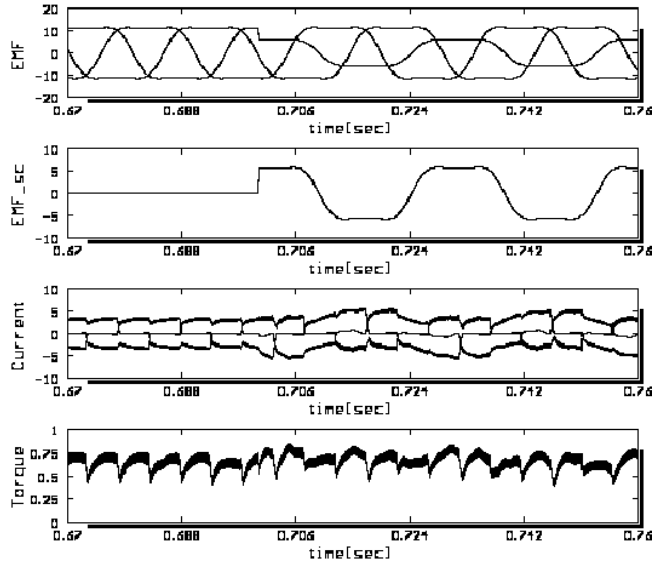

Fig. 14. Waveforms during healthy case (0.67~0.7[sec]) and 50% turn-to-turn fault case (0.7~0.76[sec]).
(a) Phase EMFs (b) Short circuit EMF (c) Phase currents (d) Torque

V. CONCLUSION

This paper presents a new approach to analyze the BLDC motor inter-turn fault by using mathematical models based on the winding function theory. By using this approach, the internal fault analysis which is one of the most difficult analyses in electric machines, can be easily performed from the self and mutual inductance calculation, without any additional tool.

The simulation results verify that the new approach is valid. The detailed phenomena of currents and torque under turn-to-turn short condition can be the guideline for early detection of internal failures in BLDC motors.

ACKNOWLEDGMENT

Authors would like to thank Dr. Ehsani and Dr. Toliyat at Texas A&M Univ. for their support.

REFERENCES

[1] Hamid A Toliyat., Thomas A Lipo., "Transient analysis of cage induction machines under stator, rotor bar and end ring faults", *IEEE Transaction on Energy Conversion*, Vol. 10, No. 2, 1999.

[2] Haylock J.A., Mecrow B.C., Jack A.G., Atkinson D.J., "Operation of fault tolerant machines with winding failures", *IEEE Transactions* on *Energy Conversion*, Vol. 14, Issue 4, pp.1490–1495, Dec. 1999.

[3] Penman J., Jiang H., "The detection of stator and rotor winding short circuits in synchronous generators by analysing excitation current harmonics", *Opportunities and Advances in International Electric Power Generation, International Conference* on (Conf. Publ. No. 419), pp.137–142, 1996.

[4] Joksimovic G.M., Penman J., "The detection of inter-turn short circuits in the stator windings of operating motors", *IEEE Transactions* on *Industrial Electronics*, Vol. 47, Issue 5, pp.1078–1084, Oct. 2000.

[5] Nandi S., Toliyat H.A., "Novel frequency domain based technique to detect incipient stator inter-turn faults in induction machines", *IEEE IAS Conference,* Vol. 1, pp.367-374., 2000.

[6] J. R. Hendershot Jr. and T.J.E Miller, Design of brushless permanent-magnet motors. *Oxford Magna Physics Publications*, ISBN 1-881855-03-1, 1994.